

Thermal fluctuations and osmotic stability of lipid vesicles

Håkan Wennerström,^{1,*} Emma Sparr,^{1,†} and Joakim Stenhammar^{1,‡}

¹*Division of Physical Chemistry, Lund University, P.O. Box 124, S-221 00 Lund, Sweden*

(Dated: July 7, 2022)

Understanding the remodeling and stability of lipid vesicles is of fundamental importance for a range of cellular processes. One crucial question is how vesicles respond to external osmotic stresses, imposed by differences in solute concentrations between the vesicle interior and exterior. Previous analyses of the membrane bending energy have predicted that spherical vesicles should become globally deformed already for nanomolar concentration differences, in contrast to experimental findings that find deformations at much higher osmotic stresses. In this article, we analyze the mechanical stability of a spherical vesicle exhibited to an external osmotic pressure in a statistical-mechanical model, including the effect of thermally excited membrane bending modes. We find that the inclusion of thermal fluctuations of the vesicle shape changes renders the vesicle deformation continuous, in contrast to the abrupt transition in the athermal picture. Crucially, however, the predicted critical pressure associated with global vesicle deformation remains the same as when thermal fluctuations are neglected, approximately six orders of magnitude smaller than the experimentally observed collapse pressure. We conclude by discussing possible sources of this persisting dissonance between theory and experiments.

I. INTRODUCTION

The absolute majority of living cells function optimally in environments with solute concentrations corresponding to an osmotic pressure close to that of physiological saline. Thus, the intracellular environment maintains an osmolarity in the range 250 to 400 mM [1, 2]. Nevertheless, cells are often exposed to osmotic stresses induced by concentration variations in the surrounding medium, and living organisms have therefore developed a range of mechanisms for coping with these variations [3, 4]. Plants and most bacteria have rigid cell walls that can sustain significant osmotic stresses. At low external osmotic pressures, excessive swelling and membrane rupture are prevented by developing an internal “turgor pressure”. For eukaryotic cells the situation is more complex: Low external osmotic pressures can here lead to membrane rupture, while high external osmotic pressures will cause the cell to shrink in volume resulting in a too crowded internal medium that will slow down metabolic processes. One strategy is to upregulate the intercellular concentration of osmotically active components such as salt or osmolytes, but this comes at a cost in metabolic energy [4]. A more direct defense against deformation or rupture due to osmotic stress is however built into the intrinsic bending energy of the cellular membrane. In order to analyse this effect, we will here consider the effect of osmotic pressure in a simplified model system consisting of a unilamellar, spherical vesicle built up by a single-component lipid bilayer.

The osmotic stability of spherical lipid vesicles has been theoretically analysed in the past [5, 6, 22], leading to the conclusion that the stabilisation against osmotic collapse due to membrane bending is negligible for all but very small (nanometre-scale) lipid vesicles, and should have no measurable effect for vesicles of sizes comparable to eukaryotic cells ($\sim 10 \mu\text{m}$). In contrast, in a recent study we experimentally measured the osmotically induced deformation of freely suspended, single-component giant unilamellar vesicles (GUVs) in this size range and found that they were able to sustain significant osmotic stresses before being deformed into a prolate shape at osmotic stresses $\Pi \gtrsim 0.15 \text{ atm}$ [7]. Upon osmotic reversal, the deformed vesicles exhibited reproducible formation of “daughter vesicles” through an endocytosis-like process in order to quickly incorporate the external medium, indicating that a sizeable bending energy ($> 10^3$ times the thermal energy) is stored in the deformed vesicles. These experimental results are broadly in line with previous experimental and computational studies on more complex, multicomponent vesicle systems, where both osmotic deformation and daughter vesicle formation have been observed [8–12]. Thus, even though neither of these studies were directly focussed on quantitatively determining the deformation threshold, the overall picture is that GUVs exhibit a significant tolerance to osmotic gradients before becoming visibly deformed from spherical shape. Motivated by this discrepancy, we here revisit the problem of the stability of spherical vesicles exposed to external osmotic stresses, taking into account the effect of thermal fluctuations of the lipid membrane. While not previously analysed in the context of osmotic stability, such thermal shape fluctuations have been extensively considered theoretically [13–18] and experimentally [19, 20] and have, among other things, been shown to promote long-ranged repulsive interactions between fluctuating lipid bilayers [13, 14]. Our analysis is based on the same basic formalism as that used in Ref. [5], expanding the thermally induced deformations in a set of fluctuation modes described by spherical harmonics. Within this framework, we

* hakan.wennerstrom@fkem1.lu.se

† emma.sparr@fkem1.lu.se

‡ joakim.stenhammar@fkem1.lu.se

derive a formally exact expression for the configuration integral Z and evaluate it analytically for the two lowest fluctuation modes. Our analysis shows that the inclusion of thermal fluctuations (i) shifts the average volume of the vesicle to lower values compared to that of the perfect sphere even for $\Pi = 0$, and (ii) changes the vesicle deformation at finite osmotic stresses ($\Pi > 0$) to a continuous one, in contrast to the athermal case. Crucially, however, the collapse of the vesicle volume appears to occur at the same value of the critical pressure Π_c as in the athermal case [5]. Thus, the inclusion of thermal fluctuations of the vesicle shape within a harmonic approximation cannot explain the significant discrepancies with experimental results, and we conclude by discussing some possible reasons for this unsettling dissonance between theory and experiments.

II. MODEL DESCRIPTION

We consider a unilamellar vesicle formed by a bilayer containing $2N_L$ lipid molecules. The area a_0 per molecule is assumed to be constant, thus making the bilayer laterally incompressible and fixing the vesicle area $A_0 = N_L a_0$; for a perfectly spherical vesicle the resulting radius is thus $R_0 = (A_0/4\pi)^{1/2}$. The general expression for the vesicle bending energy \mathcal{U}_b is given by Helfrich's expression [21]

$$\mathcal{U}_b = \int [2\kappa(H - H_0)^2 + \bar{\kappa}K]dA, \quad (1)$$

where H is the mean curvature, H_0 the spontaneous curvature, κ the bending rigidity, K the Gaussian curvature, and $\bar{\kappa}$ the saddle-splay rigidity. For a vesicle with conserved topology, the Gaussian curvature term is constant and will thus be neglected below. For a symmetric lipid bilayer, such as those composed of only a single lipid component, there is furthermore no spontaneous curvature of the bilayer. In the absence of thermal fluctuations and osmotic stresses, the stable configuration of such a vesicle is that of a perfect sphere with volume $V_0 = 4\pi R_0^3/3$, with an energy given by $\mathcal{U}_0 = 4\pi(2\kappa + \bar{\kappa})$. At finite temperatures, the vesicle shape will fluctuate around the perfect sphere, leading to an increase in the average membrane bending energy. At constant area, all such thermal excitations must thus lead to a decrease in vesicle volume, enabled by the fact that the bilayer is permeable to water. This yields an equilibrium vesicle volume $V < V_0$, determined by a balance between the bending energy of the bilayer and the entropy of the thermally excited membrane bending modes.

If the composition of the surrounding medium is changed by the addition or removal of a solute to which the bilayer is impermeable, an osmotic imbalance is created. Assuming ideal solution conditions, the induced osmotic pressure is $\Pi = kT\Delta c$, where Δc is the concentration difference, k is Boltzmann's constant, and T the temperature. If the osmotic pressure is higher inside the vesicle than outside it, corresponding to a decrease of solute concentration in the surrounding medium ($\Delta c < 0$), a tension is created in the bilayer, which eventually leads to a rupture of the vesicle. When $\Delta c > 0$, the vesicle instead has a thermodynamic driving force to shrink. If the vesicle interior has a finite solute concentration, osmotic balance will be reached when the vesicle has expelled enough water to equalise the interior and exterior solute concentrations. For the case when the vesicle contains pure solvent, the concentration can however not be equalised by a finite reduction in volume. One possibility is then that the vesicle collapses completely, thus balancing the external osmotic pressure through a direct monolayer-monolayer interaction in the collapsed state. The second option, which is the one we will consider here, is the balancing of osmotic stress by an increase in bending free energy associated with a finite volume decrease.

In Ref. [5], Zhong-can and Helfrich analysed the stability of a spherical vesicle subject to an osmotic pressure Π , using Eq. (1) for the bending energy and neglecting thermal fluctuations. They found that the vesicle remained spherical up to a critical pressure Π_c , given by

$$\Pi_c = \frac{2\kappa}{R_0^3}(6 - H_0 R_0). \quad (2)$$

For $\Pi > \Pi_c$, an instability occurs in the deformation mode with the largest wavelength, corresponding to a global deformation of the vesicle. A subsequent theoretical study by Pleiner [22] based on a weakly nonlinear stability analysis and including higher-order geometrical correction terms concluded that the deformed state corresponds to an axially symmetric, prolate shape. For a small unilamellar vesicle with $R_0 = 50$ nm and a typical bending rigidity corresponding to $20kT$, the critical pressure of Eq. (2) with $H_0 = 0$ becomes $\Pi_c \sim 8$ kPa, corresponding to $\Delta c \sim 3$ mM, indicating that vesicles in this size range can withstand non-negligible osmotic stresses without significant deformations. In contrast, a corresponding GUV with a typical radius of $R_0 = 5$ μm would withstand a pressure of only 8 mPa, corresponding to $\Delta c \sim 3$ nM, implying that almost any (deliberate or accidental) increase of the solute concentration in the external medium of a GUV suspension would lead to vesicle collapse. As discussed above, this contrasts with the general observation that spherical GUVs can be readily formed and remain stable even in chemically complex environments, and in particular with our recent observation that GUVs remain effectively spherical up to external osmotic pressures $\sim 10^6$ times larger than that predicted by Eq. (2).

For small deviations from the sphere, the instantaneous vesicle shape $R(\theta, \phi)$ can be described by an expansion in spherical harmonics $Y_{\ell m}(\theta, \phi)$ with associated coefficients $a_{\ell m}$:

$$R(\theta, \phi) = R_0 \left[1 + \sum_{\ell=0}^{\infty} \sum_{m=-\ell}^{\ell} a_{\ell m} Y_{\ell m}(\theta, \phi) \right]. \quad (3)$$

The terms with $\ell = 0$ and $\ell = 1$ correspond, respectively, to a change in average radius and a translation of the vesicle, while the terms with $\ell \geq 2$ describe the shape of the vesicle and thus determine its bending energy. The sum over ℓ is truncated above some value ℓ_{\max} set by the physical constraints of the problem, as further discussed below. To leading order in the coefficients $a_{\ell m}$, the volume and area of the deformed vesicle are given by

$$V = R_0^3 \left[\frac{4\pi}{3} \left(1 + \frac{a_{00}}{\sqrt{4\pi}} \right)^3 + \sum_{\ell m} a_{\ell m}^2 \right], \quad (4)$$

$$A = R_0^2 \left[4\pi \left(1 + \frac{a_{00}}{\sqrt{4\pi}} \right)^2 + \sum_{\ell m} a_{\ell m}^2 \left(1 + \frac{\ell(\ell+1)}{2} \right) \right], \quad (5)$$

where $\sum_{\ell m}$ implies summation over all $\ell \geq 2$ and the corresponding m . The bending energy $\Delta\mathcal{U}_b = \mathcal{U}_b - \mathcal{U}_0$ relative to the perfect sphere is furthermore given by

$$\Delta\mathcal{U}_b = \frac{\kappa}{2} \sum_{\ell m} a_{\ell m}^2 (\ell+2)(\ell+1)\ell(\ell-1) \quad (6)$$

For small deformations, we have that $a_{00}/\sqrt{4\pi} \ll 1$, and the brackets in Eqs. (4)–(5) can be expanded to leading order in a_{00} . Using the constant area constraint, the term in a_{00} in (4) can then be eliminated to yield

$$V \approx R_0^3 \left[\frac{4\pi}{3} - \frac{1}{4} \sum_{\ell m} a_{\ell m}^2 (\ell+2)(\ell-1) \right], \quad (7)$$

highlighting that any deformation of the vesicle ($a_{\ell m} \neq 0$) under the constant-area constraint necessarily leads to a *decrease* of the vesicle volume compared to that of the perfect sphere. For later developments, we reexpress (7) as an equation for the number of water molecules N in the deformed vesicle:

$$N \approx N_0 \left[1 - \frac{3}{16\pi} \sum_{\ell m} a_{\ell m}^2 (\ell+2)(\ell-1) \right], \quad (8)$$

where N_0 is the number of water molecules in the perfect sphere.

III. OSMOTIC STABILITY IN THE ABSENCE OF THERMAL FLUCTUATIONS

From Eqs. (6) and (8), it follows that the minimum energy for a given N is given by a deformation in the longest-wavelength, $\ell = 2$ modes. The corresponding bending energy $\Delta\mathcal{U}_b$ relative to the perfect sphere is given by

$$\Delta\mathcal{U}_b = 16\pi\kappa \frac{N_0 - N}{N_0} \equiv 16\pi\kappa\hat{N}, \quad (9)$$

where $\hat{N} \equiv (N_0 - N)/N_0 \in [0, 1]$ quantifies the relative deviation from spherical shape. We now create an osmotic gradient by dissolving solute in the external medium, changing the external chemical potential to $\mu_w < \mu_w^\theta$, where μ_w^θ is the chemical potential of pure water. The (free) energy change $\Delta\mathcal{U}_\mu$ relative to the pure water case associated with creating this osmotic imbalance is

$$\Delta\mathcal{U}_\mu = (\mu_w - \mu_w^\theta)(N_0 - N) = -\Pi V_w \hat{N}, \quad (10)$$

where we have used the osmotic pressure definition $\Pi V_w = (\mu_w^\theta - \mu_w)$, with V_w the molecular volume of water. By combining Eqs. (9) and (10), we note that the total energy change $\Delta\mathcal{U} = \Delta\mathcal{U}_b + \Delta\mathcal{U}_\mu$ goes negative when $(\mu_w^\theta - \mu_w) > 16\pi\kappa/N_0$, which is equivalent to the stability condition in Eq. (2) with $H_0 = 0$. Thus, due to the linear dependence on \hat{N} , for $\Pi > \Pi_c$ the vesicle can always minimise its energy by further decreasing its volume towards zero ($\hat{N} \rightarrow 1$), while for $\Pi < \Pi_c$ the minimum energy always occurs for $\hat{N} = 0$, corresponding to the perfect sphere. In the absence of thermal fluctuations, the vesicle deformation thus corresponds to a sharp transition at $\Pi = \Pi_c$ from a perfect sphere to a collapsed one, as found by Zhong-can and Helfrich [5].

IV. GENERAL EXPRESSION OF THE CONFIGURATION INTEGRAL

At finite temperature and in the absence of constraints, all the harmonic bending modes in Eq. (6) become thermally excited, and each mode contributes an average bending energy of $kT/2$. To avoid an unphysical energy divergence, an upper cutoff ℓ_{\max} to the expansion in Eq. (3) needs to be defined. The most straightforward way to estimate ℓ_{\max} is by assuming that the continuum picture of membrane deformations ceases to be relevant for wavelengths comparable to the bilayer thickness h , where $\ell_{\max} \sim R_0/h$. For typical values of $h = 5 \text{ nm}$ and $R_0 = 5 \mu\text{m}$, this estimate yields $\ell_{\max} \sim 10^3$ and a total of $\sim 10^6$ excited bending modes, since each value of ℓ corresponds to $(2\ell+1)$ degenerate modes. To account for the relation between volume and bending energy caused by the constraint of constant area A_0 , we will below treat the volume V or, equivalently, the number of enclosed water molecules, N , as a dependent variable, while ensuring that the constant-area constraint is obeyed for each individual configuration. This approach is different from previous treatments, [6, 16] which instead introduced a free energy term accounting for the area constraint using a virtual (negative) tension in the form of a Lagrange multiplier, ensuring that the constant area condition is satisfied in the mean.

In the presence of an osmotic gradient, the probability P_N of having a vesicle containing N water molecules is given by

$$P_N = \frac{Z_N \exp [\beta(N - N_0)(\mu_w - \mu_w^\theta)]}{\sum_{N'} Z_{N'} \exp [\beta(N' - N_0)(\mu_w - \mu_w^\theta)]}, \quad (11)$$

where $\beta = (kT)^{-1}$, $Z_N = e^{-\beta\mathcal{F}_b(N)}$ is the N -particle configuration integral and $\mathcal{F}_b(N)$ the corresponding bending free energy, which we define relative to the perfect sphere. Note that Z_N , and thus $\mathcal{F}_b(N)$, is independent of the osmotic stress difference, which is fully contained in the second exponential factor of (11).

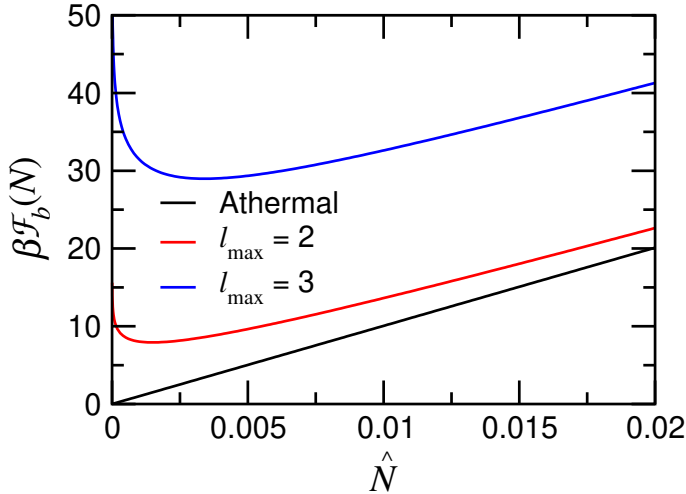


Figure 1: Bending free energy \mathcal{F}_b in the absence of osmotic stress, plotted as a function of the reduced vesicle volume \hat{N} . For the athermal case, the curve shows the linear function in (9), which is minimised for $\hat{N} = 0$. For $\ell_{\max} = 2$ and 3 , $\mathcal{F}_b(\hat{N})$ is given by the negative logarithms of Eqs. (20) and (21), respectively. Note that, as further fluctuation modes are added, the optimal volume gradually moves away from that of the perfect sphere.

To find how $\mathcal{F}_b(N)$ varies with vesicle volume, we now proceed to calculate the configuration integral Z_N . The fact that Z_N describes fluctuations at constant N , corresponding to a constant-volume constraint, introduces a coupling between the different modes through Eq. (8). We take this condition into account by introducing a δ function in Z_N , yielding

$$Z_N = \int \exp[-\beta\Delta\mathcal{U}_b(\{a_{\ell m}\})] \delta \left(C_N - \sum_{\ell m} a_{\ell m}^2 (\ell + 2)(\ell - 1) \right) \{da_{\ell m}\}, \quad (12)$$

where

$$C_N \equiv \frac{16\pi}{3} \hat{N} \quad (13)$$

is introduced to simplify notation. We now make the variable substitution $t_{\ell m} \equiv [(\ell + 2)(\ell - 1)]^{1/2} a_{\ell m}$ which

allows us to express $\Delta\mathcal{U}_b$ in Eq. (6) as a sum of two parts, where the second one only contains modes with $\ell \geq 3$:

$$\Delta\mathcal{U}_b = \frac{\kappa}{2} \left[6 \sum_{\ell=2}^{\ell_{\max}} \sum_{m=-\ell}^{\ell} t_{\ell m}^2 + \sum_{\ell=3}^{\ell_{\max}} \sum_{m=-\ell}^{\ell} (\ell^2 + \ell - 6) t_{\ell m}^2 \right]. \quad (14)$$

Since the first sum matches the argument of the δ function in Eq. (12), the configuration integral simplifies to

$$Z_N = g(\ell_{\max}) e^{-3\hat{\kappa}C_N} \times \int \exp \left[-\frac{\hat{\kappa}}{2} \sum_{\ell=3}^{\ell_{\max}} \sum_{m=-\ell}^{\ell} (\ell^2 + \ell - 6) t_{\ell m}^2 \right] \delta \left(C_N - \sum_{\ell=2}^{\ell_{\max}} \sum_{m=-\ell}^{\ell} t_{\ell m}^2 \right) \{dt_{\ell m}\}, \quad (15)$$

where $\hat{\kappa} \equiv \kappa/(kT)$, and

$$g(\ell_{\max}) \equiv \prod_{\ell=2}^{\ell_{\max}} [(\ell+2)(\ell-1)]^{-(\ell+1/2)}. \quad (16)$$

Equation (15) shows explicitly that the lowest allowed energy value is increased by $3\hat{\kappa}C_N$, yielding a higher reference value for thermal excitations as the vesicle volume is decreased. This is consistent with the analysis of the athermal case, and the value corresponds exactly to $\Delta\mathcal{U}_b$ in Eq. (9). To proceed, we note that the integrand in (15) is independent of m , and make a variable substitution to $(2\ell+1)$ -dimensional polar coordinates, with

$$\rho_{\ell} \equiv \left(\sum_{m=-\ell}^{\ell} t_{\ell m}^2 \right)^{1/2}. \quad (17)$$

After integrating over the angular coordinates, we get

$$Z_N(\ell_{\max}) = g(\ell_{\max}) h(\ell_{\max}) e^{-3\hat{\kappa}C_N} \times \int \exp \left[-\frac{\hat{\kappa}}{2} \sum_{\ell=3}^{\ell_{\max}} (\ell^2 + \ell - 6) \rho_{\ell}^2 \right] \delta \left(C_N - \sum_{\ell=2}^{\ell_{\max}} \rho_{\ell}^2 \right) \rho_2^4 \cdots \rho_{\ell_{\max}}^{2\ell_{\max}} d\rho_2 \cdots d\rho_{\ell_{\max}}, \quad (18)$$

with

$$h(\ell_{\max}) \equiv \prod_{\ell=2}^{\ell_{\max}} \mathcal{A}_{2\ell+1} = \prod_{\ell=2}^{\ell_{\max}} \frac{\pi^{\ell} 2^{\ell+1}}{(2\ell-1)!!}, \quad (19)$$

and where \mathcal{A}_n is the surface area of the unit sphere in n dimensions. The $(\ell_{\max} - 1)$ -dimensional integral in Eq. (18) represents an exact expression for the configuration integral. In the following, we will proceed to solve it for the cases $\ell_{\max} = 2$ and $\ell_{\max} = 3$ to yield explicit expressions for the free energy.

V. FREE ENERGY AND VESICLE VOLUME IN THE ABSENCE OF OSMOTIC STRESS

We first consider the case $\ell_{\max} = 2$, corresponding to the inclusion of thermal fluctuations only in the most unstable, $\ell = 2$ mode. In this case, (18) reduces to a one-dimensional integral that can readily be solved to yield

$$Z_N(\ell_{\max} = 2) = \frac{\pi^2}{24} C_N^{3/2} e^{-3\hat{\kappa}C_N}. \quad (20)$$

While also far from realistic values for GUVs, the case $\ell_{\max} = 3$ differs qualitatively from $\ell_{\max} = 2$, in that it includes the effect on the $\ell = 2$ instability from fluctuations also in the higher, $\ell = 3$ modes. In this case, the configuration integral in (18) becomes two-dimensional, and can be straightforwardly solved by subsequent integration over ρ_2 and ρ_3 to yield

$$Z_N(\ell_{\max} = 3) = \frac{\pi^6 \sqrt{10}}{9.72 \times 10^7} \frac{C_N}{\hat{\kappa}^4} e^{-\frac{9}{2}C_N\hat{\kappa}} \times \left\{ [(3C_N\hat{\kappa})^2 + 24C_N\hat{\kappa}] I_0 \left(\frac{3}{2}C_N\hat{\kappa} \right) - [(3C_N\hat{\kappa})^2 + 12C_N\hat{\kappa} + 32] I_1 \left(\frac{3}{2}C_N\hat{\kappa} \right) \right\}, \quad (21)$$

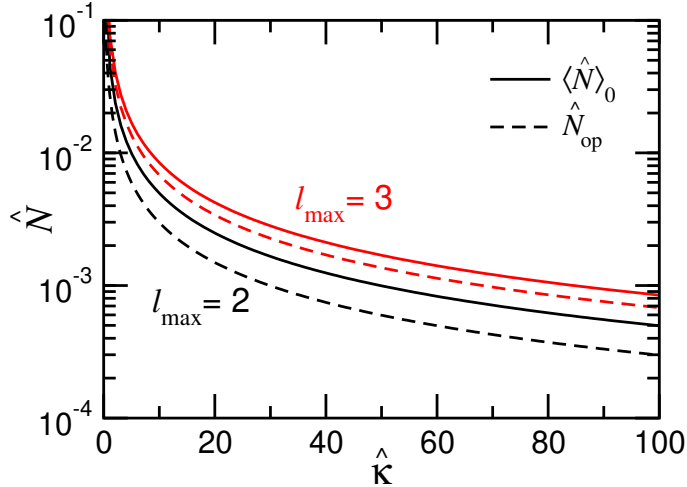


Figure 2: Average $\langle \hat{N} \rangle_0$ and optimal \hat{N}_{op} reduced vesicle size in the absence of an osmotic gradient, as a function of the reduced bending stiffness $\hat{\kappa}$.

with $I_\alpha(x)$ the modified Bessel functions of the first kind and order α . By taking the negative logarithm of Z_N in Eqs. (20) and (21), we obtain the corresponding free energies $\mathcal{F}_b(N)$ corresponding to $\ell_{\max} = 2$ and 3, shown in Fig. 1. The first obvious effect of increasing ℓ_{\max} is an increase in the total free energy, as further bending energy modes now become thermally excited. Furthermore, the minimum in free energy is gradually shifted away from the perfect sphere as more fluctuation modes are added.

From the explicit expressions for Z_N in Eqs. (20)–(21), we now quantify the deviation from spherical shape in the absence of osmotic stress by calculating the statistical-mechanical average $\langle \hat{N} \rangle_0$ using Eq. (11) with $\Pi = 0$:

$$\langle \hat{N} \rangle_0 = \frac{\int_0^1 \hat{N} Z_{\hat{N}} d\hat{N}}{\int_0^1 Z_{\hat{N}} d\hat{N}}, \quad (22)$$

where $Z_{\hat{N}}$ is the configuration integral expressed as a function of the reduced particle number \hat{N} . For $\ell_{\max} = 2$ these integrals can be solved analytically, while for $\ell_{\max} = 3$ they need to be numerically evaluated. The full expression for $\ell_{\max} = 2$ is somewhat lengthy but reduces to the following simple expression for $\hat{\kappa} \gtrsim 0.2$, which thus covers the experimentally relevant values for lipid bilayers:

$$\langle \hat{N} \rangle_0(\ell_{\max} = 2) = \frac{5}{32\pi\hat{\kappa}}. \quad (23)$$

As a consistency check, we can insert $\langle \hat{N} \rangle_0$ from (23) into (9), using the fact that all the bending energy is now located in the five modes with $\ell = 2$, to calculate the average of the bending energy $\langle \Delta\mathcal{U}_b \rangle = \frac{5}{2}kT$, just as expected from the equipartition theorem. Before we proceed, we note that $\langle \hat{N} \rangle_0$ differs from the *optimal* value \hat{N}_{op} obtained by instead minimising $\beta\mathcal{F}_b = -\ln Z_N$ with respect to \hat{N} , which gives

$$\hat{N}_{op}(\ell_{\max} = 2) = \frac{3}{32\pi\hat{\kappa}}. \quad (24)$$

The difference between Eqs. (23) and (24) goes against our standard statistical-mechanical understanding, and comes from the fact that we are far from the thermodynamic limit which here corresponds to having a large number of degrees of freedom, *i.e.*, $\ell_{\max} \rightarrow \infty$. In Fig. 2, we present the relative volume reduction \hat{N} , using both measures described above, as a function of $\hat{\kappa}$ for $\ell_{\max} = 2$ and 3. For very small values of $\hat{\kappa}$, the volume reduction is clearly too large for the harmonic approximation to be valid, while for physically relevant bending rigidities of $\hat{\kappa} \sim 20$, we get that $\langle \hat{N} \rangle_0 \approx 4 \times 10^{-3}$, corresponding to a decrease in vesicle volume of 0.4% compared to that of the perfect sphere. Finally, the results show that the discrepancy between the two volume measures indeed decreases for $\ell_{\max} = 3$ compared to $\ell_{\max} = 2$, and will eventually vanish as more fluctuation modes are added.

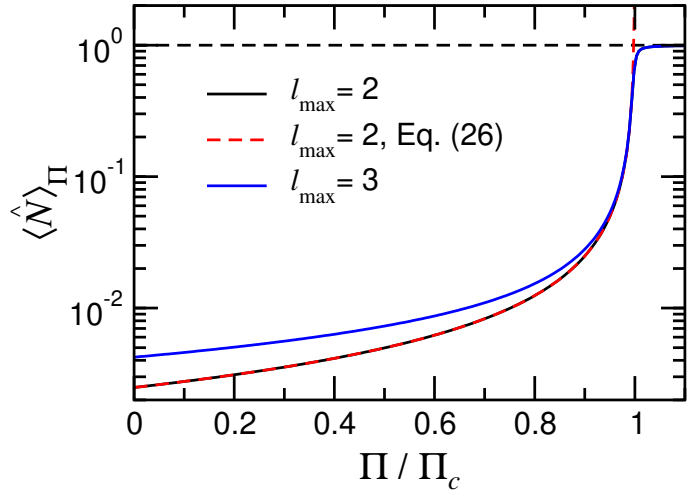


Figure 3: Average reduced vesicle size $\langle \hat{N} \rangle_\Pi$ for $\hat{\kappa} = 20$ in the presence of an osmotic gradient Π , obtained from Eq. (25). Note that the inclusion of thermal fluctuations makes the vesicle deformation increasingly gradual, while not affecting the location of the vesicle collapse, which is still given by Π_c in (2). The red dashed line shows the simplified expression (26), valid for $\Pi \lesssim \Pi_c$, while the solid lines correspond to an exact evaluation of Eq. (25). The dashed line for $\hat{N} = 1$ corresponds to the fully collapsed vesicle.

VI. VESICLE DEFORMATION DUE TO OSMOTIC STRESS

We now turn to the case of a constant osmotic imbalance $\Pi > 0$ across the membrane, corresponding to a higher solute concentration outside than in the vesicle interior. In the presence of such an osmotic stress, reexpressing Eq. (11) as a function of Π , the average volume changes to

$$\langle \hat{N} \rangle_\Pi = \frac{\int_0^1 \hat{N} Z_{\hat{N}} \exp(\beta \hat{N} \Pi V_0) d\hat{N}}{\int_0^1 Z_{\hat{N}} \exp(\beta \hat{N} \Pi V_0) d\hat{N}}. \quad (25)$$

For $\ell_{\max} = 2$, the integrals can once more be analytically evaluated, leading to the following generalisation of Eq. (23):

$$\langle \hat{N} \rangle_\Pi(\ell_{\max} = 2) = \frac{5}{32\pi\hat{\kappa}} \frac{\Pi_c}{\Pi_c - \Pi}, \quad (26)$$

where Π_c is still given by the athermal value in Eq. (2) and the simplified expression is valid in the dual limit $\hat{\kappa} > 1$ and $\Pi < \Pi_c$. This indicates that, for $\ell_{\max} = 2$, thermal fluctuations do not affect the location of the instability compared to the athermal case, but changes the nature of the transition from abrupt to continuous. The picture does not change qualitatively when one includes also the $\ell = 3$ modes in the description, where we instead numerically evaluate Eq. (25), leading to the results shown in Fig. 3. Compared to the $\ell_{\max} = 2$ case, the volume change is now more gradual and shifted towards lower values of Π . Strikingly, however, the position of the global vesicle deformation remains at $\Pi = \Pi_c$ given by the athermal condition (2) even when fluctuations in $\ell = 3$ modes are included. Thus, it appears that the correlation between fluctuations in the most unstable mode and higher modes does not affect the athermal instability criterion, a result which is likely to hold for arbitrary values of ℓ_{\max} . This is true in spite of the fact that, when thermally exciting higher bending modes, the energy can be stored in all available modes rather than in only the $\ell = 2$ modes themselves. Such fluctuations however change the nature of the transition from abrupt to continuous: in the absence of an osmotic stress, the average vesicle volume is only marginally affected by thermal fluctuations, while for $\Pi \approx \Pi_c$ the effect of thermal fluctuations can be sizeable. Thus, the effect of an osmotic stress is to “soften” the bending modes, making them significantly more excited than for $\Pi = 0$.

VII. DISCUSSION

By explicitly considering the effect of thermal shape fluctuations, we have shown that spherical vesicles subject to an external osmotic pressure respond in a continuous way by gradually decreasing their volume, in contrast to

the abrupt instability in the absence of thermal fluctuations. The vesicle volume formally goes to zero at a well-defined critical pressure Π_c identical to the one first derived by Zhong-can and Helfrich for the athermal case [5]. As noted above, this value is many orders of magnitude smaller than the experimentally observed one, indicating that the theoretical description does not include all relevant aspects of the problem. To conclude, we will thus discuss a few possible sources of this significant discrepancy between theory and experiments.

1. While exact within the harmonic approximation, one limitation of our treatment is that, as Π approaches Π_c , the vesicle volume gradually decreases beyond the point where the assumption of small deviations from spherical shape implicit in Eqs. (3)–(8) becomes invalid. Thus, strictly speaking, the harmonic energy expression of Eq. (6) does not cover the experimentally relevant parameter space, suggesting that additional terms should be introduced into the model in order to quantitatively describe the significant deformations at $\Pi \approx \Pi_c$. These terms can come from two different sources: Firstly, Eqs. (7) and (8) are valid only to leading order in the amplitudes $a_{\ell m}$. There are thus higher order geometrical corrections to the expressions for the vesicle free energy. Secondly, Eq. (1) is based on a series expansion of the bending energy. Using the planar state as reference, one expects also a fourth-order term with a positive coefficient [15]. Considering that the bending modes become highly excited under osmotic stress, such terms might give significant contributions to the bending energy. However, the fourth-order bending effects are inversely proportional to A_0 [15] and are thus expected to be most important for small vesicles.
2. The presence of a concentration difference between the interior and exterior regions of the vesicle creates an asymmetry which gives rise to a nonzero spontaneous curvature $H_0 < 0$ due to solute-bilayer interactions [23, 24], even for the case where the vesicle itself is fully symmetric, leading to an increase of Π_c according to Eq. (2). However, the value of Π_c corresponds to extremely low concentrations, so that the asymmetry, and thus the spontaneous curvature contribution to the bending energy, should be negligible around Π_c . However, in the presence of some other stabilising mechanism, this spontaneous curvature term might become important for the osmotic pressures where GUVs are experimentally observed to be stable. According to (2), this effect is expected to be more important for GUVs than for small vesicles, since it scales as $R_0 H_0$.
3. All the results are based on the assumption that the lipid bilayer is laterally incompressible, corresponding to constraining the fluctuations to a constant area A_0 . While a good approximation, this is not strictly the case and an external osmotic pressure will induce a finite reduction also of the area. Since stretching elasticities K_A of lipid membranes are typically large (~ 50 mJ/m²), the coupling between membrane contraction and osmotic pressure leads to a stabilisation of the spherical vesicle relative to the constant-area case. To leading order, the relative area change $\hat{A} = (A - A_0)/A_0$ should be proportional to the pressure and inversely proportional to K_A . By dimensional analysis we furthermore expect that $\hat{A} \sim R_0$, implying that the effect should become significant for large vesicles.

Thus, while the present work provides important insights into the physics of shape fluctuations in vesicles under osmotic stress, significant future work is required to analyse to what extent the additional effects discussed above can contribute to reduce or eliminate the discrepancy between theory and experiment, and to further shed light on the role of bending energy as a stabilising mechanism against osmotic stress in biological systems.

VIII. ACKNOWLEDGEMENTS

JS kindly acknowledges funding from the Swedish Research Council (grant ID 2019-03718).

[1] H. Wennerström, E. V. Estrada, J. Danielsson, and M. Oliveberg, *Proc. Natl. Acad. Sci. USA* **117**, 10113 (2020).
[2] M. Oliveberg and H. Wennerström, *QRB Discovery*, Accepted (2022).
[3] E. Bremer and R. Krämer, *Annu. Rev. Microbiol.* **73**, 313 (2019).
[4] J. M. Wood, *J. Gen. Physiol.* **145**, 381 (2015).
[5] O.-Y. Zhong-can and W. Helfrich, *Phys. Rev. Lett.* **59**, 2486 (1987).
[6] U. Seifert, *Adv. Phys.* **46**, 13 (1997).
[7] X. Liu, J. Stenhammar, H. Wennerström, and E. Sparr, *J. Phys. Chem. Lett.* **13**, 498 (2022).
[8] J. Pencer, G. F. White, and F. R. Hallett, *Biophys. J.* **81**, 2716 (2001).
[9] W. Zong, Q. Li, X. Zhang, and X. Han, *Colloids Surf. B* **172**, 459 (2018).
[10] T. Bhatia, T. Robinson, and R. Dimova, *Soft Matter* **16**, 7359 (2020).
[11] C. Vanhille-Campos and A. Šarić, *Soft Matter* **17**, 3798 (2021).
[12] S. U. A. Shibly, C. Ghatak, M. Abu Sayem Karal, M. Moniruzzaman, and M. Yamazaki, *Biophys. J.* **111**, 2190 (2016).

- [13] W. Helfrich, *Z. Naturforsch.* **33a**, 305 (1978).
- [14] W. Helfrich and R. Servuss, *Il Nuovo Cimento D* **3**, 137 (1984).
- [15] W. Helfrich, *J. Phys. France* **47**, 321 (1986).
- [16] S. T. Milner and S. A. Safran, *Phys. Rev. A* **36**, 4371 (1987).
- [17] I. Bivas and N. S. Tonchev, *Phys. Rev. E* **100**, 022416 (2019).
- [18] T. V. S. Krishnan, K. Yasuda, R. Okamoto, and S. Komura, *J. Phys.:Condens. Matter* **30**, 175101 (2018).
- [19] J. Oberdisse and T. Hellweg, *Adv. Colloid Interface Sci.* **247**, 354 (2017).
- [20] I. Hoffmann, C. Hoffmann, B. Farago, S. Prévost, and M. Gradzielski, *J. Chem. Phys.* **148**, 104901 (2018).
- [21] W. Helfrich, *Z. Naturforsch. C* **28**, 693 (1973).
- [22] H. Pleiner, *Phys. Rev. A* **42**, 6060 (1990).
- [23] A. Kabalnov, U. Olsson, and H. Wennerström, *J. Phys. Chem.* **99**, 6220 (1995).
- [24] R. Ghosh, V. Satarifard, A. Grafmüller, and R. Lipowsky, *ACS Nano* **15**, 7237 (2021).